POLITECNICO
MILANO 1863

SCUOLA DI INGEGNERIA INDUSTRIALE
E DELL'INFORMAZIONE

Executive Summary of the Thesis

Laser Pulse Amplification and Characterization studies at the High Power Laser Facility of ESRF

Laurea Magistrale in Physics Engineering - Ingegneria Fisica

Author: Matteo Masto

Advisor: Prof. Giacomo Claudio Ghiringhelli

Co-advisor: Dr. Nicolas Sévelin - Radiguet

Academic year: 2020-2021

1. Introduction

In recent years the scientific interest towards matter extreme conditions of pressure and temperatures has grown and so did the technologies employed to study such exotic states. A still poorly known phase of matter, called Warm Dense Matter, in between the solid and plasma states, is dominant in many compounds subjected to temperatures above 10,000 K at densities in between 10^{-2} to 10 g/cm^3. The validation with experimental data of theoretical models of such state would be crucial for the fields of planetary science, fundamental condensed matter studies, industrial applications and Inertial Confinement Fusion.
One of the most used methods to achieve GPa pressures and tens of thousands of Kelvin degrees is the laser driven dynamic compression. This approach, which involves the use of high power laser pulses to generate compression waves propagating through the sample, is currently adopted for the experiments conducted at the High Power Laser Facility (HPLF) of ESRF. There, samples are probed with synchrotron radiation to obtain, through XAFS spectra, information on the evolution of their internal structure during the compression [1]. Beside laser pulse energy and spatial intensity distribution, it is known that the type of compression (steady shock, decaying shock or ramp) produced in the sample is mostly dependent on the its time duration and intensity temporal profile.[2].
Within this framework, the work summarized here aimed at studying the temporal distortion caused by the amplification for the specific case of the HPLF and the optimal compensation of such distortions for any desired target shape and energy.
Furthermore, the adaptation to our specific case and the installation of the Passive Pulse Replication System, conceived by Marciante *et al.* in 2007 [3], has been carried out. This last project was aiming at improving the quality of the measurements of the drive laser temporal profile, thus allowing users to use this cleaner and more reliable shape as input for hydrodynamic simulations of the specific compression experiment.

2. HPLF description

The solid state laser employed at the HPLF is the Premiumlite100 produced by ©Amplitude company. It is a Nd:Glass (1053 nm) able to deliver nanosecond pulses of the order of 100 joules. The seed source is generated inside the ©iXBlue

ModBox Front End where the temporal profile is shaped in fiber components. The nanojoule pulse, now in free space propagation, is then amplified through different stages using flash-lamps pumped Nd:Glass rods and disks. Firstly a Regenerative Amplifier (RGA) increases the pulse energy up to 10 mJ through multiple passages before the Pockels cell switch. Then a double pass through a ϕ 5mm diameter rod (D5) and another double pass through two ϕ 25mm diameter rods (D25) brings the energy to 15 J at maximum power. The last amplification stage consists in two double passages through four disk amplifiers (P100) for a final theoretical output energy of 100 J.

3. Laser pulse amplification and seed reconstruction

A common effect with high-fluence pulses of appreciable time duration is that during the passage through the amplifier the gain medium suffers a significant depletion of the inverted population caused by the first temporal portion of the beam; thus the trailing edge experiences a damped gain. The result is a temporal distortion of the intensity profile. This effect, called *gain saturation* is well described by the Frantz-Nodvik equations [4]:

$$I(z,t) = \frac{I_0(t-\frac{z}{v})}{\left[1-\left[1-exp\left\{-\sigma_s \int_0^z N_0(z)dz\right\}\right]exp\left\{-\frac{2}{\Gamma_s}\int_{-\infty}^{t-\frac{z}{v}} I_0(t')dt'\right\}\right]} \quad (1)$$

$$N(z,t) = \frac{N_0(z)exp\left\{-\sigma_s \int_0^z N_0(z)dz\right\}}{\left[exp\left\{\frac{2}{\Gamma_s}\int_{-\infty}^{t-\frac{z}{v}} I_0(t')dt'\right\}+exp\left\{-\sigma_s \int_0^z N_0(z)dz\right\}-1\right]} \quad (2)$$

These coupled equations, derived from the 4-levels systems rate equations, relate the instantaneous intensity of a travelling pulse with the population inversion distribution in the medium along the propagation direction once the initial conditions of I_0 and N_0 are given. Main parameters are the saturation fluence Γ_s, the stimulated emission cross-section σ_s.

The implementation of these equations into a conceived Python based script allowed for the simulation of the amplification and temporal distortion of the laser pulse. For this scope other aspects as spatial filtering and spot-size changes throughout the whole chain have been considered in the simulation. Initial values of the population inversion distribution, initially unknowns, have been tuned accordingly to obtain the best fit of the simulated temporal profile with the measured one.
Moreover, a self-consistent iterative process has been developed for the reconstruction of the seed pulse shape and energy for a given target shape and energy. It is based on the backward run of the target pulse, transformed at each passage by the reversed Frantz-Nodvik equations, down to the seed that is then used as new input. The convergence, depending on the tolerance and on the initial guess shape is achieved in less than one second, after ≈ 15 iterations.

3.1. Results

The pulse shapes obtained from the simulation, for a 10 ns top-hat target of 100 J out of the P100, with the mentioned intermediate energies, are depicted below.

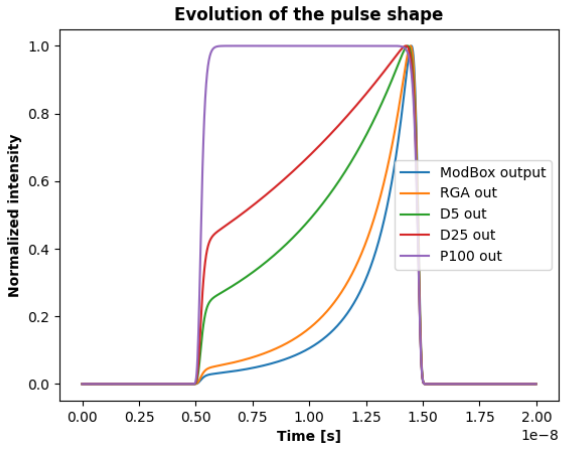

Figure 1: Simulated temporal profiles through the amplification stages to compensate the gain saturation effect and produce a top-hat final shape.

A better insight of the script capabilities is obtained when the amplification is simulated starting from the *measured* ModBox output, and measured temporal shapes and energies for successive stages are compared.

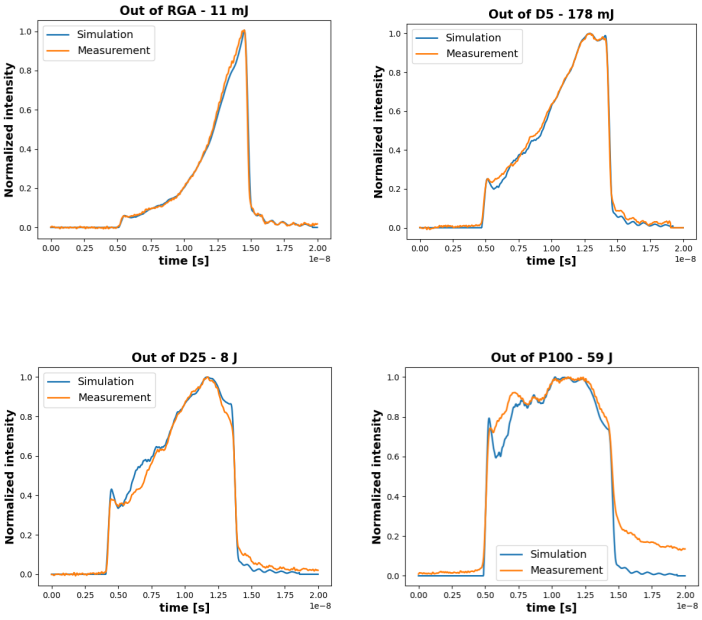

Figure 2: Comparison between simulation and measurements of the temporal profile out of each amplification stage. Measured energies were respectively 10.6 mJ, 150 mJ, 8.8 J and 55 J. The input shape of the simulation was the measurement of the seed profile out of the ModBox.

The agreement between measurements and simulation results is quite good for all the cases. The main mismatch is in the first halves of the pulse, where the exponential gain is prevailing over the saturated one. In this region noisy fluctuations of the input signal are over-amplified in the simulation. Moreover, the main hypothesis accounting for the actual smaller height of the first spike is that its intensity gets cut by the transient in the Pockels cells transmissivity window switching. Energies obtained for such temporal shapes are in agreement with the measured ones. Higher values found are indeed expected, meaning that for real cases significant energy losses occur.

4. Energy estimation from temporal measurements

The presented results of the simulation have been obtained using as ModBox output pulse energy a quantitative estimation retrieved from its temporal measurement. Indeed, not knowing this energy from direct measurement, due to lack of proper instrumentation, it would have been a further unknown parameter of the simulation.
Thus all the pipeline from the fiber, passing through the photodiode, to the oscilloscope has been modeled with conversion factors and the sources of power losses.

$$E_{in} = \frac{10^{\theta}}{R_{\lambda} R_{load}} \left(\int_{\tau}^{\tau+\tau_p} V_{osc} dt - \frac{\tau_p}{\tau} \int_{0}^{\tau} n_{osc} dt \right) \quad (3)$$

The energy, given by 3, depends on the photodiode responsivity R_{λ}, on the load resistance R_{load}, on the sources of losses θ, and on the integral of the voltage signal cleaned of the electrical noise. The main unknown losses, in the θ term, concerned the fiber-photodiode coupling, the fiber-fiber connection and the eventual free space- fiber injection. Different measurements have been taken with different configurations of fibers and connectors and a least square problem for the linear over-determined system of the form has been set.
The solution was obtained with ®MATLAB function for constrained linear least squares problems and bonds of 0 and 10 dB were given respectively for lower and upper limits of loss terms. Results are reported in Table 1.

ModBox output pulse energy	5.6711 nJ
ModBox fiber - photodiode coupling	6.5516 dB
Normal fiber - photodiode coupling	5.2644 dB
ModBox fiber - normal fiber	7.5519 dB
Normal fiber - fiber coupling	0.7984 dB
Absence of AR	0.0 dB
Free space - fiber coupling	2.6618 dB

Table 1: Least squares solution for the unknown term of losses and ModBox output energy

Residuals absolute values are below 0.5 dB, within the variability, translated in dB, of every voltage measurement with respect to its average over 6 recordings.
Obtained value of the energy is in agreement with the expected as well as the loss values for each case. Smaller active area of the photodiode with respect to the fiber core diameter is the main source of loss together with the connection between two different types of fiber. Only exception is the zero amount of losses due to the absence of AR coating, clearly forced by the constraints. However, also recorded voltages were unexpectedly lower for fibers equipped with AR coating with respect the others.

5. Passive Pulse Replication System

As mentioned in the Introduction, this technique allows to improve significantly the signal-to-noise ratio (SNR) of temporal profile measurements through the average of many exact replicas of the single pulse. It is particularly suited for single-shot experiments, as in our case, for which it is impossible to make averages with measurements of other shots, but on the other hand a high SNR is required.
The system mainly consists in a structure made of optical fibers of different lengths and optical couplers. Once a bounce of photons from the single pulse is injected into a fiber, the idea is to make it run through a series of optical couplers that are able to split the incoming pulse into two identical parts of half the initial power each, and make them travel through two different paths. It is clear that, if a proper delay is introduced between the two outgoing branches of each coupler, i.e. extending the length of one of them with the help of optical fiber, the splitted pulses will not overlap when passing through the subsequent couplers, allowing for the creation of a *train* of ideally identical pulses.

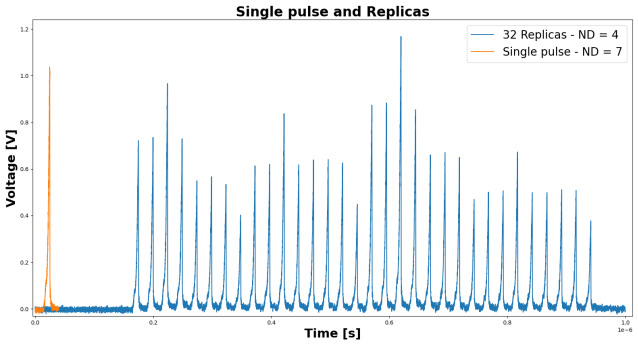

Figure 3: Train of replicas at the photodiode. Different amplitudes of the replicas peaks depend, in principle, on the number of connectors and fiber length each pulse has passed through, which are the main causes of energy loss.

Looking at time for which the cross-correlation function of the first replica with respect to the train is maximum, it is possible to know exactly the delays among replicas, to slice the train accordingly and to perform the average.
In our case we produced a train of 32 replicas and managed to obtain their peak power average almost equal to the peak of the single shot measurement.

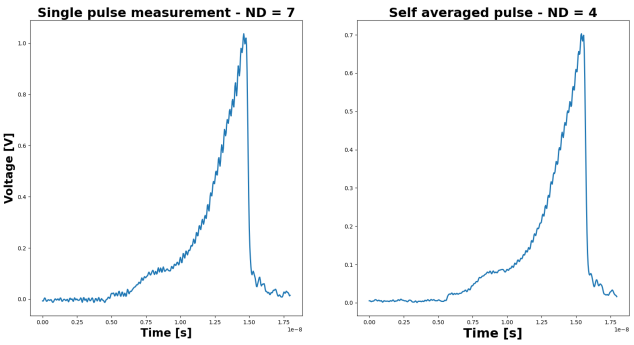

Figure 4: Effect of the self-average of 32 replicas on the SNR. For the single pulse a ND filter of 7 was required not to saturate the photodiode, while using the PPRS, that due to multiple splitting of the incoming pulse lowers the peak power to the photodiode, it was reduced to 4.

The improvement of the quality of the measurement is clearly visible especially in the first temporal region. However, the calculated SNR did not improved by a factor $\sqrt{32}$ as expected when averaging stochastic variables, even using the same signal for the two SNR calculations. One hypothesis for this disagreement may be the not perfect randomness of the noise in each sliced replica. Indeed, due to photodiode discharge current the temporal region among replicas still might contain some signal, while the baseline before the arriving of the single pulse is truly random. This would explain the lower SNR trend *vs* the number of replicas considered, with respect to the theoretical one.

6. Conclusions

The implementation of the Frantz-Nodvik equations into a computer simulation designed for the specific case of the HPLF of ESRF, produced results of energies and temporal profiles of the drive laser in good agreement with measurements. This is crucial for the monitoring and the shaping of the laser pulses in each stage. It will be helpful for estimating and individuating the major sources of losses, and the possibility to retrieve the optimal compensated seed shape represents is an useful tool for users and beamline operators to obtain the desired target shapes. However, important further developments can be done, starting from a complete modeling of

the ModBox in order to be able to put hands on its digital inputs rather than only check its optical output.
The estimated energy of the ModBox output will be soon compared with the actual one obtained with a direct measurement, and this would offer the possibility to refine the proposed pipeline model, and exactly tune the initial population inversion for each amplifier. By now the current estimation is however able to confirm the the suspects of loss of power raised by ©Amplitude laser engineers.
To conclude, the installation at the Facility of the PPRS is an important upgrade for the laser diagnostic. Besides the benefit produced by the self-average, such system makes possible to exploit all the optical power that the fiber system can withstand without the risk of damaging, to increase the signal over the noise level of the oscilloscope. This in principle allows to maximize its potentiality adding more couplers and fibers to the present system, up to the point at which the maximum voltage peak of the train is right below the saturation threshold of the photodiode for an optical power input of the single pulse right below the damage threshold of the fiber.

7. Acknowledgements

My acknowledgements go firstly to my Advisor Prof. Ghiringhelli for giving me the opportunity to develop my thesis work at the ESRF. At the same way, I want to thank my Supervisor at the ESRF, Dr. Nicolas Sévelin-Radiguet, who carefully guided me from the beginning of the internship, supporting me, clarifying my doubts and teaching me a lot. A big thank goes also to Prof. Gianluca Valentini for sharing his opinions with me about section 4.
A warm thanks goes also to all the staff of the beamline ID24 and my office mates at ESRF.

References

[1] N. Sévelin-Radiguet, R. Torchio, G. Berruyer, H. Gonzalez, S. Pasternak, F. Perrin, F. Occelli, C. Pépin, A. Sollier, D. Kraus, A. Schuster, K. Voigt, M. Zhang, A. Amouretti, A. Boury, G. Fiquet, F. Guyot, M. Harmand, M. Borri, J. Groves, W. Helsby, S. Branly, J. Norby, S. Pascarelli, and O. Mathon, "Towards a dynamic compression facility at the ESRF," *Journal of Synchrotron Radiation*, vol. 29, pp. 167–179, Jan 2022.

[2] T. S. Duffy and R. F. Smith, "Ultra-High Pressure Dynamic Compression of Geological Materials," *Frontiers in Earth Science*, vol. 7, 2019.

[3] J. R. Marciante, W. R. Donaldson, and R. G. Roides, "Averaging of Replicated Pulses for Enhanced Dynamic-Range Single-Shot Measurement of Nanosecond Optical Pulses," *IEEE PHOTONICS TECHNOLOGY LETTERS*, vol. 19, pp. 1344–1346, 2007.

[4] L. M. Frantz and J. S. Nodvik, "Theory of Pulse Propagation in a Laser Amplifier," *Journal of Applied Physics 34*, pp. 2346–2349, 1963.